Topo-Bathymetric Lidar Survey and Hydrodynamic Modelling Analysis of River Philip, Nova Scotia

Nova Scotia Community College
Applied Geomatics Research Group
NSCC, Middleton, NS
Tel. 902 825 5475
Email: timothy.webster@nscc.ca

The Confederacy of Mainland Mi'kmaq

Lily Priest
Project Lead (River Philip)
Department of Aquatic Resources and Fisheries Management
The Confederacy of Mainland Mi'kmaq

March 31st, 2024

How to cite this work and report:

NSCC Applied Geomatics Research Group. 2024. Topo-Bathymetric Lidar Survey and Hydrodynamic Modelling Analysis of River Philip, Nova Scotia. Technical Report delivered to Internal Services Department, Government of Nova Scotia, Applied Geomatics Research Group, NSCC Middleton, NS.

Executive Summary

The Nova Scotia Community College's Applied Geomatics Research Group (NSCC-AGRG) collaborated with The Confederacy of Mainland Mi'kmaq (CMM) to conduct a survey of River Philip, stretching from the Town of Oxford upstream to Collingwood Corner. The technology employed by NSCC-AGRG was a Leica Chiroptera 4X airborne topo-bathymetric lidar sensor mounted on a fixed-wing manned aircraft. The survey was executed on October 20th, 2023, and was timed to coincide with ideal weather conditions and a near-base flow river stage.

The survey generated several data products, including a highly detailed 50 cm digital elevation model (DEM) and digital surface model (DSM), alongside a 5 cm orthophoto mosaic captured by an RCD30 camera. NSCC-AGRG developed hydrodynamic models using DHI MIKE 21 software to simulate River Philip's hydrodynamics across a spectrum of flow scenarios, from low to high flow conditions.

Results from the models offer insights into identifying areas within the river vulnerable to drying, potentially impeding fish passage. These findings can provide guidance to CMM for directing their efforts towards river restoration.

Table of Contents

Table of Figures

List of Tables

Introduction

Project Background

Topo-bathymetric lidar operates by deploying both near-infrared (NIR) and green lasers from an aircraft, typically in an elliptical or circular scan pattern (Anderson, et al., 2017). These lasers measure the time taken for their pulses to travel to and from various surfaces, including land, water, and the seabed (Axelsson, 1999). The NIR laser pulse reflects off the land or water, while the green laser pulse partially reflects at the air-water interface and undergoes refraction, with the remainder passing through the water column and reflecting off the seabed before returning to the detector (Anderson, et al., 2017).

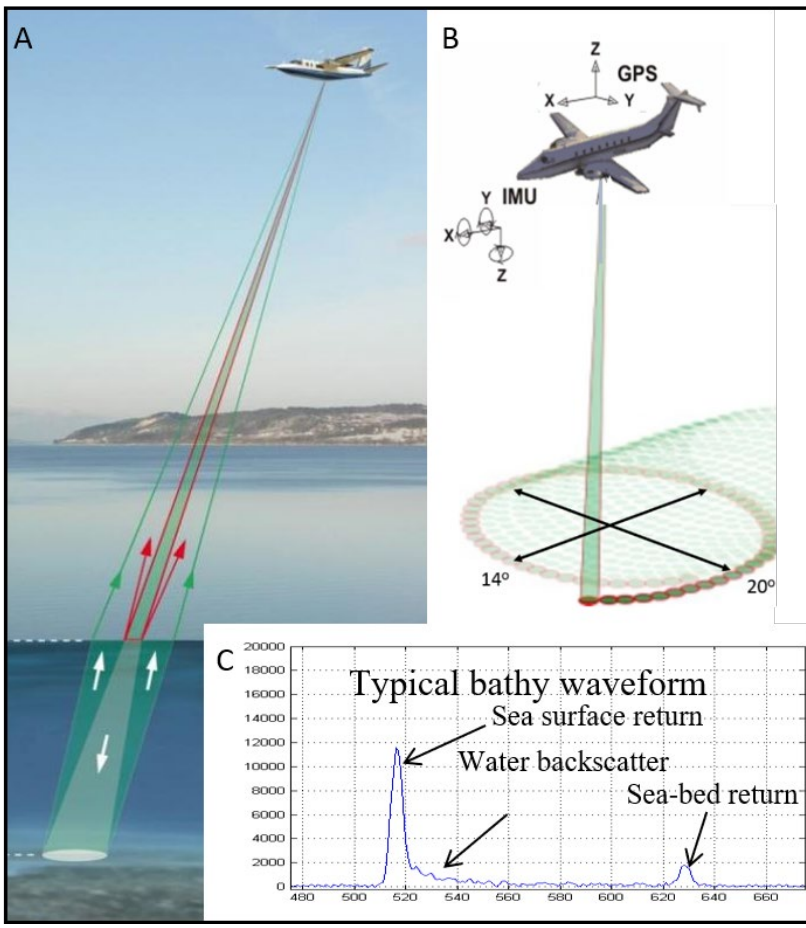

Figure 1. A) Interaction of the NIR and green laser light when travelling between air and water, refraction and scattering take place; B) Typical elliptical scan pattern for topo-bathymetric lidar with navigation system; C) Typical waveform captured from the green laser. Figure obtained from Leica, n.d.

The path of the green laser becomes intricate as it transitions from air to water, where the speed of light decreases by approximately 1/3 due to refraction. Within the water column, the green light scatters and gradually loses energy with depth until it reflects off the sea or riverbed and returns to the detector (Szafarczyk & Toś, 2023). To account for the change in the speed of light and the refraction angle from air to water, the system must accurately detect the water surface to compensate for these optical path effects. The NIR laser typically exhibits a beam divergence around 0.5 mrad, whereas the green laser exhibits a larger beam divergence of approximately 3 mrad (Xu, et al., 2021).

Unlike sonar, where the speed of sound in water is significantly affected by salinity and temperature, topo-bathymetric lidar works equally well in fresh or saltwater. However, the water clarity is typically the limiting factor for a successful topo-bathymetric lidar survey (Szafarczyk & Toś, 2023). The reflectance of seabed or river-lakebed also plays a role in addition to water clarity for determining how deep the green laser can penetrate and reflect to the sensor (Wang, et al., 2023).

The NSCC-AGRG own and operate a Leica Chiroptera 4X (CH4X) high-resolution topo-bathymetric lidar scanner equipped with an ancillary Leica RCD30 60-megapixel multispectral (RGB-NIR) camera that can survey seabed morphology and habitat, including submerged vegetation (Webster, et al., 2019). More recently, AGRG has been conducting surveys over rivers to test the applicability of the sensor to provide riverbed depth and morphology that can aid in fish passage and fish habitat studies (Webster, Ferris, McGuigan, & Laskey, 2022).

Purpose of Study

Through several river stewardship and monitoring initiatives, CMM oversees species-at-risk in various rivers throughout mainland Nova Scotia. Their monitoring efforts have enabled comprehensive assessments of Atlantic Salmon population and distribution within River Philip, alongside the identification of Brook Floater populations. Additionally, CMM has implemented temperature monitors and conducts water quality assessments to detect and address any potential issues concerning water quality within the River Philip watershed.

CMM enlisted the services of NSCC-AGRG to conduct a topo-bathymetric lidar survey with the purpose of generating a digital elevation model (DEM) covering segments of the River Philip main stem, as well as sections of two of its tributaries: Little River and Black River. Additionally, NSCC-AGRG was tasked with creating a hydrodynamic model for the surveyed sections.

Prior to conducting their topo-bathymetric lidar survey, NSCC-AGRG carried out reconnaissance in River Philip to evaluate water clarity and determine the suitability of the proposed area of interest (AOI) for surveying. Upon visually inspecting the Black River and Little River tributaries, as well as conducting Secchi disk measurements along various sections of these tributaries, it became evident that the high turbidity levels would adversely affect the laser's ability to accurately capture the riverbed elevation (Figures 2A and B). Consequently, a new survey AOI was proposed and agreed upon with CMM, focusing the survey on the River Philip main stem, where water clarity conditions were more favourable (Figure 2C). The updated AOI and aircraft survey lines are depicted in Figure 3.

Figure 2. Assessment of water clarity conditions. A) Little River; B) Black River; and C) River Philip main stem.

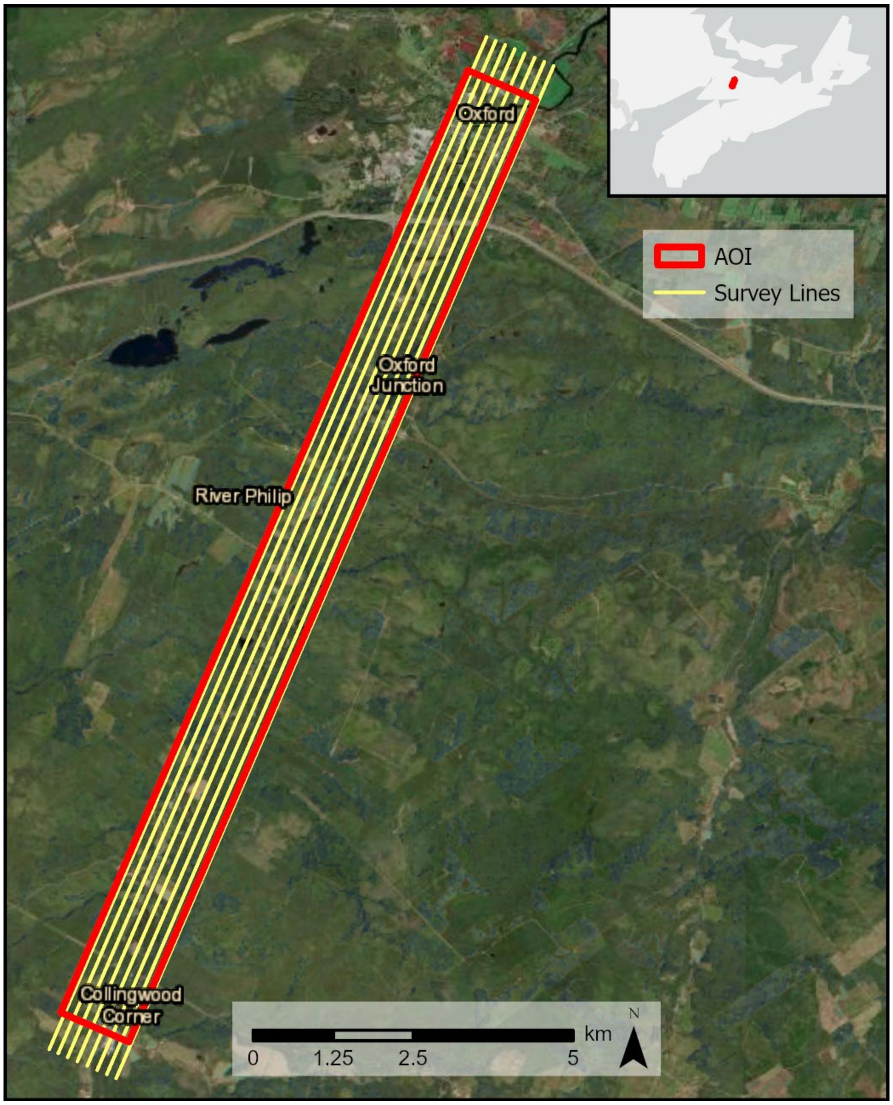

Figure 3. Extent of River Philip main stem surveyed with CH4X topo-bathymetric lidar scanner and RCD30 camera.

Methods

Methods on survey preparation, sensor management, field sampling and data processing are detailed in the following sections.

Sensor Specifications and Installation

The lidar sensor utilized for this survey was the Leica Chiroptera 4X, an integrated topographic-bathymetric lidar sensor equipped with a 60-megapixel Leica RCD30 multispectral camera. This sensor employs a 1064 nm near-infrared laser to map ground and sea surface positions at a frequency of 500 kHz, while a green 515 nm laser is utilized to map bathymetric positions at 35 kHz. Operating in an elliptical scanning pattern, the lidar captures data from various angles, minimizing shadow effects and reducing sensitivity to wave interference compared to lateral "saw-tooth" scanners. Simultaneously, the Leica RCD30 camera captures multispectral motion-compensated imagery.

The bathymetric laser's ability to penetrate the water column is contingent upon water clarity, with the system boasting a depth penetration rating of approximately 1.5 times the visible extinction (Secchi depth).

NSCC-AGRG collaborated with Eastern Topographics to charter a Cessna 206 single-engine aircraft capable of accommodating the lidar unit. The CH4X sensor was installed in the aircraft in Debert, NS, and underwent calibration on October 18th, 2023, over a ground control site established by NSCC-AGRG in Truro.

Data Collection

Survey lines were planned out using Leica Mission Pro, maintaining a flight altitude of 400 m and a speed of 65 m/s, with a 30% lateral overlap to guarantee seamless coverage without any data gaps. The survey mission commenced from the Debert airport, and the study area was surveyed on October 20th, 2023. To ensure precise georeferencing, the active control station located in Bible Hill/Truro served as the GNSS base station.

Weather conditions were monitored to mitigate the risk of significant wind events before or during the survey, as they have the potential to disturb water turbidity by agitating sediment within the water column. It is important to highlight that wind’s impact on river water is relatively minor compared to coastal waters, where wave action is more prominent. Additionally, rainfall conditions were closely observed to ensure that water levels remained close to base flow, minimizing the distance the green laser had to travel between the water surface and the riverbed to obtain accurate elevation data (Figure 4). Low water levels in the river also coincide with more exposed topography, eliminating the need to account for refraction in the elevation values.

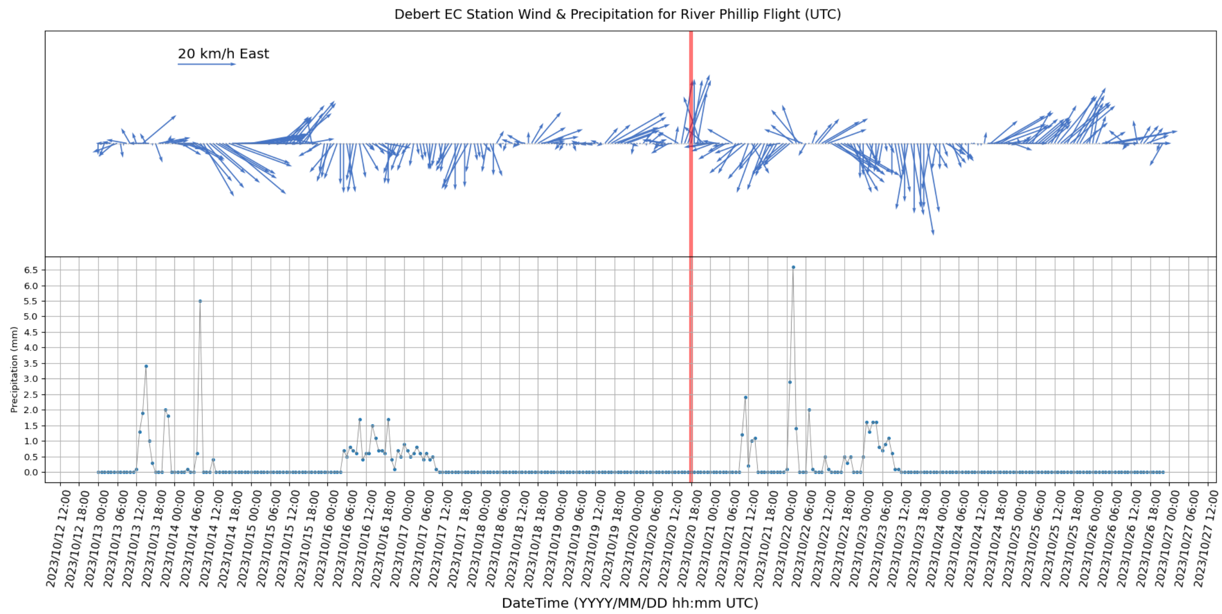

Figure 4. Wind and precipitation data sourced from Environment Canada's Debert weather station before, during, and after the CH4X topo-bathymetric lidar survey. The flight duration is depicted by the red line.

The Water Survey of Canada's flow gauge, situated in the Middle River, Pictou, served as the closest gauged river to River Philip (Figure 5). This gauge was closely monitored to track water levels in the area.

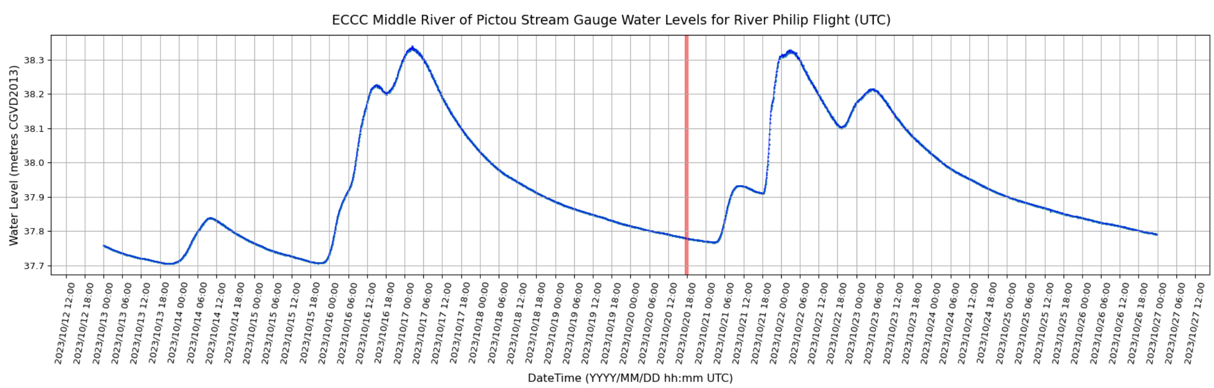

Figure 5. Water level (m CGVD2013) of the Middle River in Pictou before, during, and after the CH4X topo-bathymetric lidar survey. The red line indicates the duration of the flight.

Lidar Data Processing

A smoothed trajectory of the lidar and camera positions was calculated by linking system GNSS positions and IMU attitude with the control data from nearby stations using NovAtel Inertial Explorer. Leica Lidar Survey Studio (LSS) was used to process CH4X waveforms to discrete georeferenced (NAD83 CSRSv7) points by linking laser returns to the processed aircraft trajectory to produce point clouds in the LAS format. The data were inspected to ensure there was sufficient overlap (30%) and the AOI was fully covered by lidar returns. LAS files were read into Bentley Terrascan to analyze and further refine point metrics. Points were classified into discrete classes based on their physical characteristics including relative geometry and reflective properties (Table 1).

Table 1. Lidar point classification values and descriptions.

Classification Value	Meaning
1	Unclassified
2	Ground
4	Medium vegetation
7	Low point (noise)
9	Topographic water surface
18	High noise
40	Bathymetric point
41	Bathymetric water surface
42	Derived water surface
80	Bathymetric vegetation

Two data products were directly derived from the lidar point cloud: 1) a rasterized digital elevation model (DEM), providing a seamless representation of the ground above and below the water surface, excluding trees, buildings, and other surface objects; and 2) a rasterized digital surface model (DSM), encompassing both ground and surface features.

Image Processing

Multispectral RCD30 imagery was processed using Agisoft Metashape Professional. The processed smooth trajectory was linked to image events based on system time tags. This linkage was used to define the exterior orientation (EO) for each of the RCD30 images where camera position (x, y, z) and attitude (yaw, pitch, roll) were recorded for every exposure with positional accuracies better than 0.01 m and rotational accuracies better than 0.004 degrees. Any ambiguity between relief displacement and lens distortion was solved by using a well-defined internal orientation (IO) of the engineered zero RCD30 lens during the camera boresight process at the Truro calibration site. Captured imagery was positioned using an aerial triangulation model where possible to generate the best relief map for subsequent orthorectification.

Hydrodynamic Model Processing

Surface Generation

NSCC-AGRG employed the DHI suite of tools, which incorporates the MIKE 21 2D Flow Model for hydrodynamic simulation and processing. The DEM produced by NSCC-AGRG during their 2023 River Philip survey was merged with GeoNova lidar datasets to extend coverage across a broader area of the River Philip watershed for modeling purposes. The resulting raster was then resampled to 3 metres.

Model Simulation

Hydrodynamic simulations were driven using discharge conditions along the upstream boundary of the model, collected by NSCC-AGRG during their 2012 study of River Philip hydrodynamics and related flood risk. Discharge measurements were collected using a Valeport electromagnetic (EM) flow meter or a Valeport suspended impeller flow meter, depending on safety requirements related to river stage. The method of flow calculation was the same for both units; flows were recorded under a bridge on Water Street perpendicular to the river orientation at a 2 m sampling interval (Webster, Crowell, McGuigan, & Collins, 2012). Model simulations were conducted to replicate river hydrodynamics, utilizing four discharge observations at 3.95 m^3/s, 6.43 m^3/s, 13.63 m^3/s, and 46.24 m^3/s. Table 2 lists the parameters that remained constant across all simulation runs.

Table 2. Parameters used for the Mike 21 Flow Model hydrodynamic models.

Parameter	Value
Start Time	2011-01-01 12:00:00 AM
End Time	2011-01-02 12:00:00 PM
Time Step Interval	2 s
Number of Time Steps	64,800
Courant Number	2.19
Drying Depth	0.05 m
Wetting Depth	0.1 m
Eddy Viscosity (Flux-Based)	2 m^2/s
Bed Resistance (Manning Formulation)	25 $m^{1/3}/s$

Results

Lidar Products

Two data products were derived directly from the lidar point cloud, 1) a rasterized digital elevation model (DEM) which is a continuous representation of the ground above and below the water surface, devoid of trees, buildings, and other surface objects, and 2) a rasterized digital surface model (DSM) which captures both ground and surface features. Topographic and bathymetric data were of high quality and exhibited very little noise, which resulted in smooth elevation models.

Once the seamless DEM and DSM were built, colour shaded relief (CSR) maps were generated for the survey area that can be used to interpret the relief in the area (Figure 6; Figure 7).

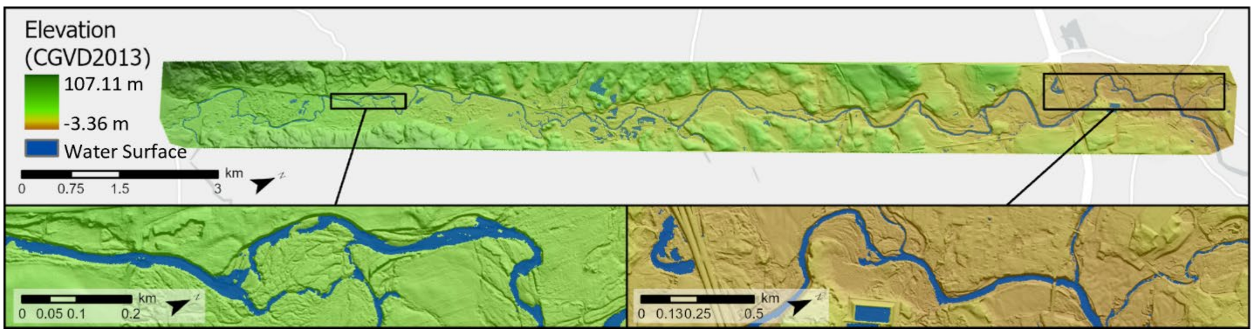

Figure 6. Digital elevation model of River Philip displayed as a colour shaded relief with the water surface captured during the time of flight as an overlay.

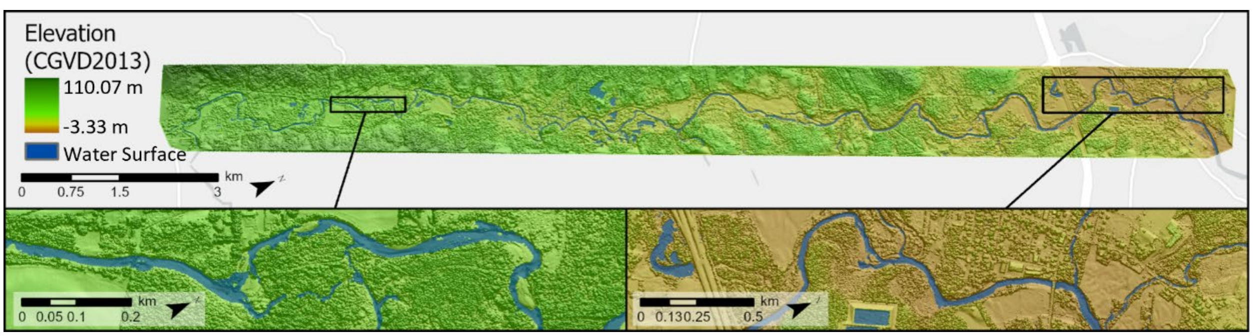

Figure 7. Digital surface model of River Philip displayed as a colour shaded relief with the water surface captured during the time of flight as an overlay.

The topo-bathymetric sensor gauges the water surface utilizing returns from both the green and NIR lasers. These data sets are then utilized to establish a "modeled" water surface, aiding in calibrating the refraction angle and the change in the speed of light as it transitions from air to water and back to the sensor. After deriving the water surface, it undergoes refinement, and once deemed appropriate, the elevations of the water surface are subtracted from the DEM surface to formulate a water depth map (Figure 8).

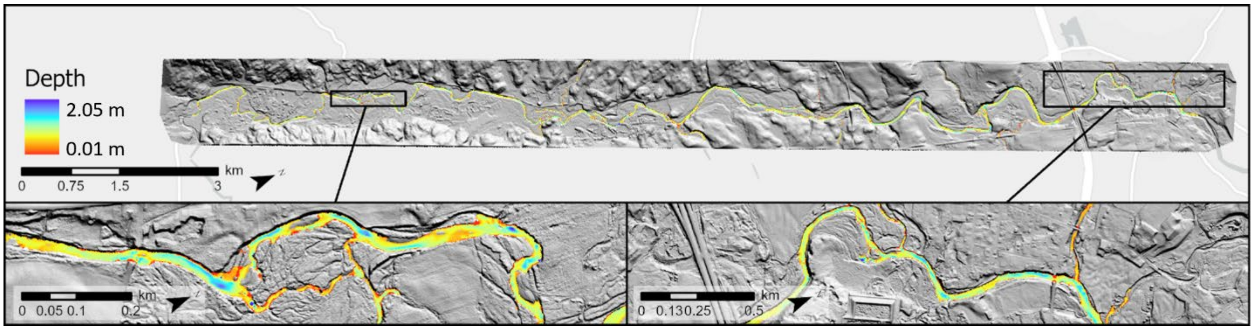

Figure 8. Depth map of River Philip captured during time of flight. The depth layer is overlaid on a hillshade of the digital elevation model.

Image Products

The orthophoto mosaic product was generated at a resolution of 5 cm with pixel perfect alignment between frames and covered the entire extent of the AOI (Figure 9).

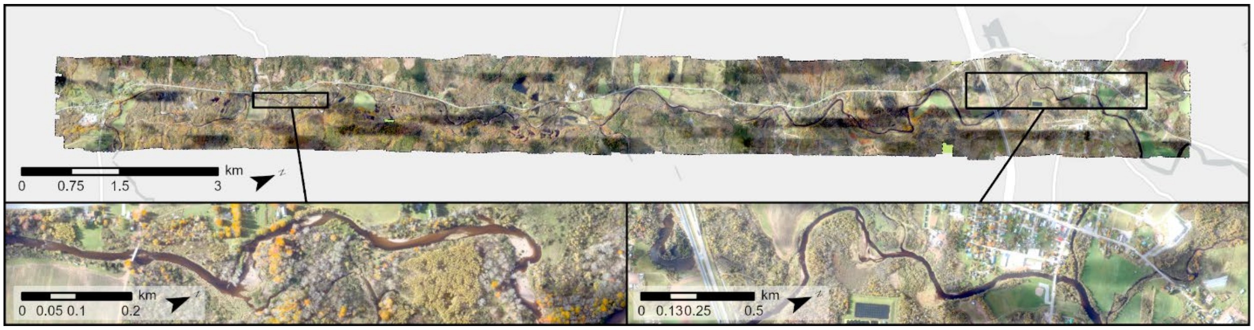

Figure 9. Orthophoto mosaic of River Philip captured by NSCC-AGRG's RCD30 camera.

Hydrodynamic Model Products

Water Depth

At a designated time-series extraction point near the Water Street Bridge along River Philip, water depth was monitored throughout various flow level model simulations. After approximately fourteen hours of model run-time, the water depths stabilized. Specifically, in ascending order of flow, the model depths stabilized at 0.32 m, 0.44 m, 0.72 m, and 1.57 m.

Figure 10 illustrates the water depths derived from the MIKE 21 hydrodynamic model at the Water Street Bridge in Oxford, with different discharge levels set as boundary conditions within the model.

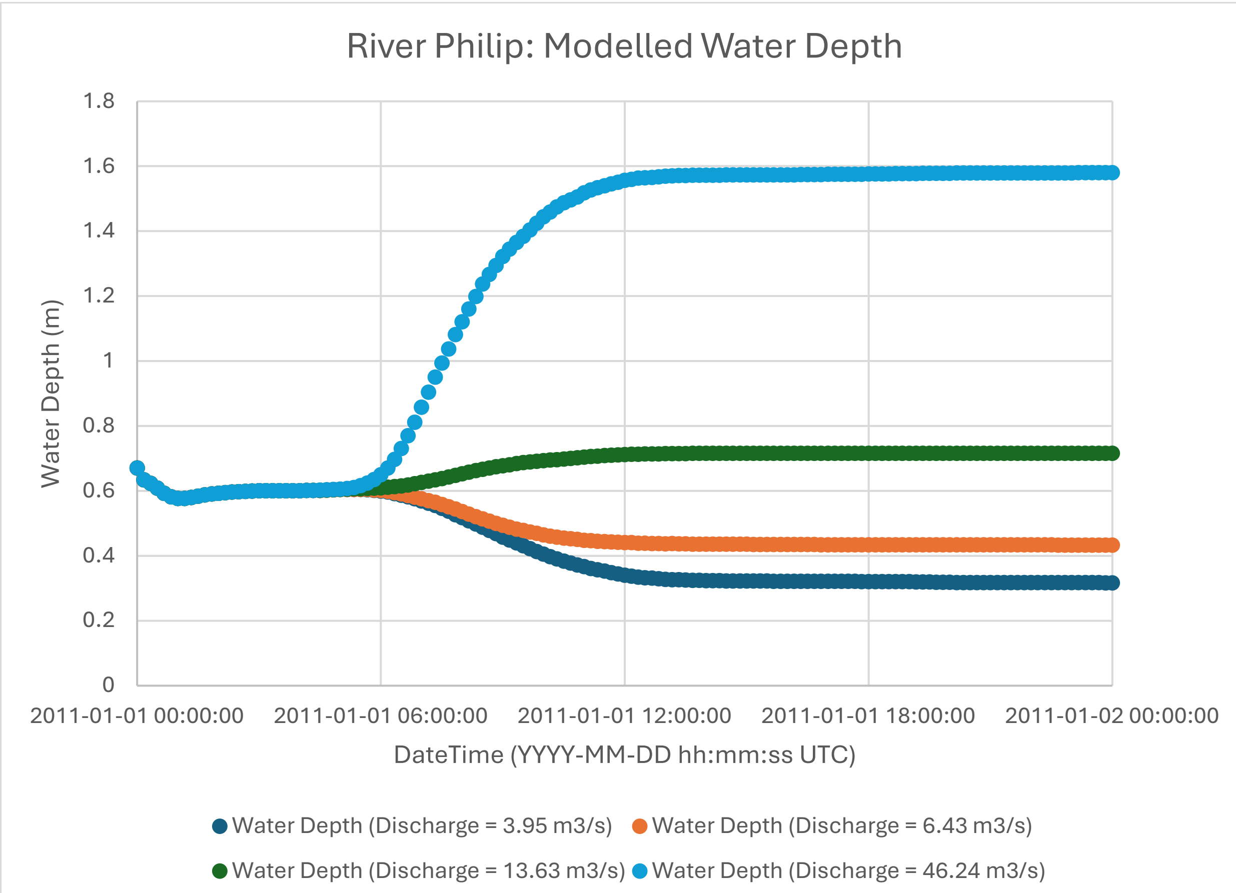

Figure 10. Water depths derived from the MIKE 21 hydrodynamic model at Water Street Bridge in Oxford, with different discharges set as boundary conditions within the model.

Depth grids were generated from each model scenario at the time step when water depth stabilized at the time-series extraction point (Figure 11-Figure 14). In the first three model simulations, where discharge conditions ranged from 3.95 m^3/s to 13.63 m^3/s, there was a transition in maximum depth from 1.77 m to 3.03 m. Notably, these scenarios exhibited a relatively similar inundation extent, with water levels remaining below the riverbank (Figure 11-Figure 13). Conversely, the model scenario with a discharge set at 46.24 m^3/s resulted in a maximum depth of 3.51 m and a notably larger inundation extent compared to earlier models, with modeled water levels surpassing the riverbank (Figure 14).

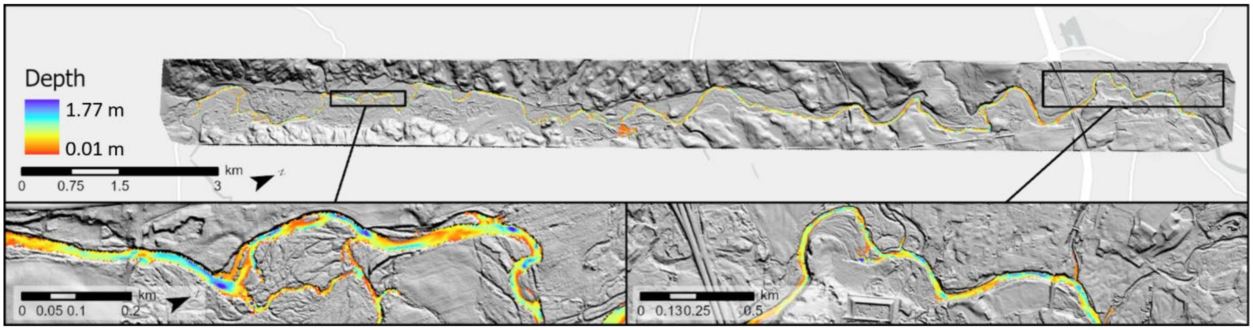

Figure 11. Modelled water depth of River Philip with a discharge value of 3.95 m^3/s set as a boundary condition.

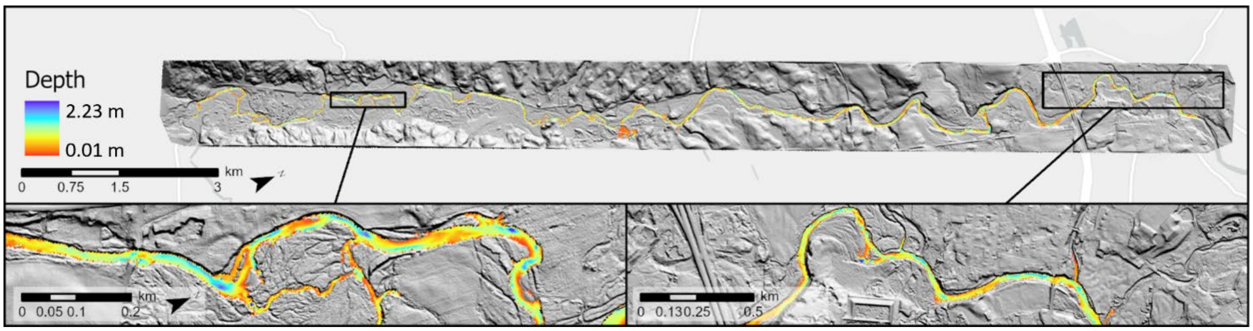

Figure 12. Modelled water depth of River Philip with a discharge value of 6.43 m^3/s set as a boundary condition.

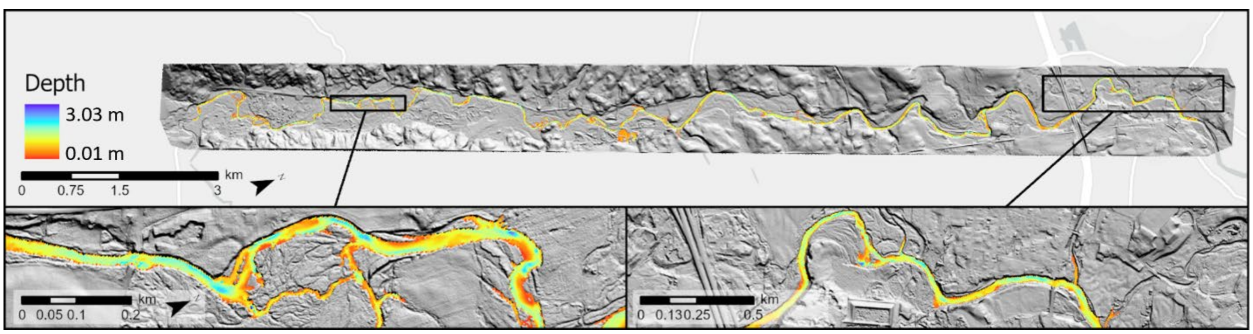

Figure 13. Modelled water depth of River Philip with a discharge value of 13.63 m^3/s set as a boundary condition.

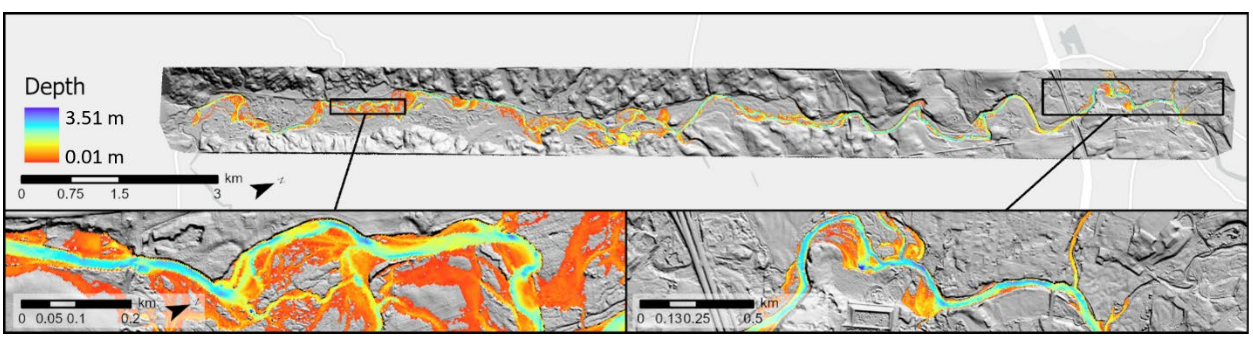

Figure 14. Modelled water depth of River Philip with a discharge value of 46.24 m^3/s set as a boundary condition.

Discussion

The results derived from the topo-bathymetric lidar survey of River Philip hold particular significance to CMM, given their vested interest in the river stemming from their species-at-risk monitoring efforts focused on Atlantic Salmon and Brook Floater populations.

The high-resolution DEM and DSM datasets obtained from the survey provide essential information for CMM's habitat assessment and conservation initiatives aimed at safeguarding these vulnerable species. By accurately delineating river morphology and hydrodynamic processes, including water depth variations and habitat complexity, the lidar-derived data offer valuable insights into the ecological requirements and habitat preferences of Atlantic Salmon and Brook Floaters.

The detailed bathymetric data and water depth maps derived from the hydrodynamic model facilitate the identification of critical spawning habitats, rearing areas, and migration corridors essential for the survival and reproductive success of these species. By pinpointing areas of suitable habitat and potential barriers to fish passage, such as shallow riffles or submerged obstacles, CMM can prioritize conservation efforts and implement targeted restoration measures to enhance habitat quality and connectivity along the river.

Additionally, the orthophoto mosaic product generated from the survey provides a visual depiction of the riverine landscape, allowing for detailed land cover classification and vegetation mapping. This information aids in identifying riparian zones, wetland habitats, and other ecologically sensitive areas crucial for supporting healthy aquatic ecosystems and sustaining biodiversity.

Conclusion

The results of the lidar survey provide valuable tools and resources for CMM to make informed decisions regarding habitat management and conservation planning initiatives in the River Philip watershed. Utilizing the insights gained from the survey data allows CMM to actively contribute to the conservation and protection of species-at-risk populations, including Atlantic Salmon and Brook Floaters, ensuring their preservation for future generations.

References

Anderson, M., Gergely, A., Al-Hamdani, Z., Steinbacher, F., Larsen, L., & Ernsten, V. (2017). Processing and performance of topobathymetric lidar data for geomorphometric and morphological classification in a high-energy tidal environment. *Hydrol. Earth Syst. Sci, 21*(1), 43-63.

Axelsson, P. (1999). Processing of laser scanner data - algorithms and applications. *ISPRS Journal of Photogrammetry and Remote Sensing, 54*(2-3), 138-147.

Szafarczyk, A., & Toś, C. (2023). The Use of Green Laser in LiDAR Bathymetry: State of the Art and Recent Advancements. *Sensors, 23*(1), 292.

Wang, J., Wang, L., Feng, S., Peng, B., Huang, L., Fatholahi, S., . . . Li, J. (2023). An Overview of Shoreline Mapping by Using Airborne LiDAR. *Remote Sensing, 15*(1), 253.

Webster, T., Crowell, N., McGuigan, K., & Collins, K. (2012). *Integrated River and Coastal Hydrodynamic Flood Risk Mapping.* Report comissioned by Atlantic Climate Adaptation Solutions Association (ACASA).

Webster, T., Ferris, K., McGuigan, K., & Laskey, E. (2022). *Topo-Bathymetric Lidar survey and analysis of the Stewiacke River, NS.* Nova Scotia Community College - Applied Geomatics Research Group. Technical report.

Webster, T., Macdonald, C., McGuigan, K., Crowell, N., Lauzon-Gray, J., & Collins, K. (2019). Calculating macroalgal height and biomass using bathymetric LiDAR and a comparison with surface area derived from satellite data in Nova Scotia, Canada. *Botanica Marina*.

Xu, W., Guo, K., Liu, Y., Tian, Z., Tang, Q., Dong, Z., & Li, J. (2021). Refraction error correction of Airborne LiDAR Bathymetry data considering sea surface waves. *International Journal of Applied Earth Observation and Geoinformation, 102*, 12.